PRVO: Probabilistic Reciprocal Velocity Obstacle for Multi Robot Navigation under Uncertainty

Bharath Gopalakrishnan[1], Arun Kumar Singh[2], Meha Kaushik[1], K. Madhava Krishna[1] and Dinesh Manocha[3]

Abstract— **We present PRVO, a probabilistic variant of Reciprocal Velocity Obstacle (RVO) for decentralized multi-robot navigation under uncertainty. PRVO characterizes the space of velocities that would allow each robot to fulfill its share in collision avoidance with a specified probability. PRVO is modeled as chance constraints over the velocity level constraints defined by RVO and takes into account the uncertainty associated with both state estimation as well as the actuation of each robot. Since chance constraints are in general computationally intractable, we propose a series of reformulations which when combined with time scaling based concepts leads to a closed form characterization of solution space of PRVO for a given probability of collision avoidance. We validate our formulation through numerical simulations in which we highlight the advantages of PRVO over the related existing formulations.**

I. Introduction

Computing collision free-trajectories for multiple robots is a challenging but important problem that finds application in robotics and, swarm and crowd simulations. Approaches like [2], [3], which are built on the concept of velocity obstacles (VO) [1] solves this problem in a decentralized manner using local navigation techniques. The computational complexity of these approaches stems from the non-convexity of the collision avoidance constraints formulated in the velocity space of the robots. Some faster techniques use a convex approximation of collision avoidance constraints at the expense of working with a reduced set of collision-free velocities [4].Most algorithms for multi-robot navigation focus primarily on the deterministic setting, where it is assumed that each robot can perfectly estimate the states of the neighboring robots and execute the computed avoidance maneuver without any errors. In reality, however, both the actuation and the state estimation associated with a robot tend to be imprecise and it is important to take this uncertainty into consideration while computing avoidance maneuvers.In this paper, we present a novel algorithm for multi-robot collision avoidance that explicitly takes into account, the perception, as well as the actuation uncertainty of each robot, i.e the uncertainty associated with error between the computed and executed avoidance maneuver. Our approach combines ideas from velocity obstacle based multi-robot collision avoidance and chance constraints which are used to ensure constraint satisfaction under uncertainty [5], [6]. These chance constraints ensure that the probability of a constraint being satisfied is greater than a specified threshold.

Contributions and Main Results The primary contribution of the proposed work lies in construction and efficient solution of chance constraints defined over first order collision avoidance conditions like Reciprocal Velocity Obstacle (RVO). We characterize the resulting set of inequalities as Probabilistic Reciprocal Velocity Obstacle or PRVO. On the algorithmic side, we present a novel Bayesian decomposition to isolate and highlight the individual effects of position and velocity level uncertainty (both resulting from state estimation and actuation) on the distribution of PRVO. To put it in simpler terms, we relate how much of the position and velocity level uncertainty is avoided for a given probability of collision avoidance. We further build on these insights and combine it with the idea of time scaling based decomposition of dynamic collision avoidance constraints to obtain a closed-form characterization of solution space of PRVO for a given probability of collision avoidance. The computational complexity of PRVO depends on the algebraic form of the probability distribution used to model the uncertainty. For the Gaussian distribution model, we show that the computational complexity of PRVO is comparable to its deterministic counterpart and involves solving single variable quadratic inequalities.

On the implementation side, we present simulation results validating the proposed formulation and highlighting effect of uncertainty parameters on PRVO. We also show that PRVO based collision avoidance significantly outperforms bounding volume based approaches [16], [17] in terms of arc length (20% reduction) and traversal time (33% reduction) of the resulting trajectories. Finally, we also empirically evaluate how the relationship between RVO and VO which exists in the deterministic setting gets transformed in the probabilistic setting.

Layout The rest of the paper is organized as follows. Section II contrasts the proposed formulation with the existing works in terms of the uncertainty model used and the approach followed for modeling dynamic collision avoidance under uncertainty. Section III-A summarizes the notations used in the paper. Section III presents the collision avoidance conditions as modeled through Reciprocal Velocity Obstacle (RVO) in the deterministic setting. Section IV introduces the model of the uncertainty used in the current work followed by the introduction of chance constraints over the inequalities defined by RVO. Section V presents a series of time scaling based reformulations of the computationally intractable chance constraints. We present simulation results

[1] RRC, IIIT-Hyderabad, [2] ATMRI, School of MAE, NTU, Singapore, [3] University of North Carolina, Chappel Hill. The research is supported in part by ARO grant W911NF- 14-1-0437 and NSF grant 1305286. The second author is supported by grant ATMRI:2014-R6-PHAM awarded by NTU and the Civil Aviation Authority of Singapore

in section VI, in which among other things we also highlight the advantages of the proposed formulation over prior work.

II. Related Work

Uncertainty Model: We model uncertainty in our formulation as Gaussian random variables, characterized by their mean and covariance matrices. Many existing works like [7]-[10], [16],[17] use similar models. However among these, [7]-[9], [16], [17] considers the effect of only state estimation uncertainty while treating the robot as a deterministic entity. Algorithms presented in [10] consider the effect of both perception and motion uncertainty but only in the context of dynamic collision avoidance of a single robot.

Dynamic Collision Avoidance: It is possible to model dynamic collision avoidance using the methods designed for static obstacles. The key idea is to integrate velocities of each robot and model collision avoidance between the resulting position level trajectories. It is possible to define chance constraints over these class of constraints to incorporate the effect of state-estimation as well as actuation uncertainty [11], [12], [13]. The key point to note here is that the resulting chance constraints would explicitly depend on only the distribution of position level uncertainty of the robots and consequently would be simpler than those presented in the proposed work. However, purely position level constraints do not appropriately capture the dynamic collision avoidance behavior. To understand this further, consider a pair of robots whose footprints at current position do not overlap and thus purely position level constraints would classify them as collision free. The fact that their current velocities might lead them to collision in some future time horizon is irrelevant.

The above discussed limitations can be removed by modeling dynamic collision avoidance as a first order constraint like RVO [2] which explicitly depends on the both position and velocity variables. Existing approaches to incorporate uncertainty in such first order constraints can be found in [17], [16] which rely on increasing the size of the robot depending upon the covariance of the position and velocity uncertainty. An alternative approach is presented in [7] where, chance constraints defined over velocity obstacle is solved through discretization of the reachable velocity space of all the robots and subsequent exhaustive search. The proposed work differs from [7] in terms of technical approach followed which leads to a more efficient closed-form characterization of collision free velocities. The proposed work is also a major improvement over our earlier work [15] which only considered the effect of state estimation uncertainty and thus entailed a much simpler formulation.

III. Background

A. Symbols and Notations

We used bold-faced small case letters with superscripts to describe vectors associated with a particular robot. For example, the position and velocity of robot i is represented as $\mathbf{p}^i = (p_x, p_y)$ and $\mathbf{v}^i = (v_x, v_y)$, respectively. We use $f^{RVO^i_j}$ to represent the collision avoidance conditions computed using the RVO formulations over the velocity space of each robots. The symbol $\mathbf{v}^i_{rvo}$ represents collision avoiding velocities modeled through deterministic RVO. We use μ and Σ with suitable subscripts and superscripts to represent mean and variance of a distribution. We use $E[.]$ and $Var[.]$ to define expectation and variance of a function with respect to random variable arguments. In section III-C and V, we use an additional superscript "s" to denote time scaled variants of vectors, functions or constraints.

B. Reciprocal Velocity Obstacle

In this section, we briefly review the concept of Reciprocal Velocity Obstacle (RVO). We do not go into detail, but rather just present the general algebraic form for the collision avoidance constraints defined by RVO, which is sufficient for understanding the ideas presented in this paper. For details, refer to [2]. We consider disc- shaped robots each modeled as following single integrator system, $\dot{x}^i = v^i_x, \dot{y}^i = v^i_y$.

Consider a collision scenario in which two robots with radii R^i and R^j are moving with constant velocities $\mathbf{v}^i$ and $\mathbf{v}^j$. RVO allows each robot to independently compute an avoidance maneuver by inferring the other robot's current position and velocity. There are two quintessential features of RVO. First, each robot employs same kind of rotation to avoid collisions, i.e each robot either employs clockwise or anticlockwise rotation. The exact amount of rotation or in other words the exact collision avoiding velocity is defined by the following inequality, where, $\mathbf{v}^i_{rvo}$ represents the velocity which allow robot i to come out of RVO with respect to current trajectory of robot j.

$$f^{RVO^i_j}(\mathbf{p}^i, \mathbf{p}^j, \mathbf{v}^i, \mathbf{v}^j, \mathbf{v}^i_{rvo}) \geq 0. \tag{1a}$$

$$f^{RVO^i_j}(.) = \|\mathbf{r}^{ij}\|^2 - \frac{((\mathbf{r}^{ij})^T(2\mathbf{v}^i_{rvo} - \mathbf{v}^i - \mathbf{v}^j))^2}{\|2\mathbf{v}^i_{rvo} - \mathbf{v}^i - \mathbf{v}^j\|^2} - (R^{ij})^2. \tag{1b}$$

$$\mathbf{r}^{ij} = (x^i - x^j, y^i - y^j)^T, \quad R^{ij} = R^i + R^j. \tag{1c}$$

It is easy to see that (1a) is a non-convex quadratic with respect to $\mathbf{v}^i_{rvo}$ and thus, computing a characterization of its solution space and consequently collision free velocities automatically becomes an expensive problem. In the next section, we describe how time scaling based concepts can be used to significantly reduce the computational burden.

C. Time Scaled Based Simplification of RVO Constraints

1) Time Scaling Definition: Time scaling allows one to compute different velocity profiles for a given geometric path. To put it formally, suppose, a robot i chooses a velocity $\mathbf{v}^i$ which takes it along a trajectory X^i, in some time interval $(t_0 \;\; t_c)$. Let the position at time t_c while moving along this trajectory be $\mathbf{p}^i$. Now, changing the velocity to $s\mathbf{v}^i$ for some $s > 0$, will ensure that the robot moves along the same path as that associated with the trajectory X^i, but now in a different time scale. In other words, the same point $\mathbf{p}^i$ will now be reached by the robot at a different time say t_{c1}. Refer [19] for further reading on time scaling.

2) Solving RVO constraints with Time Scaling Concepts: The central idea is to let each robot guess a necessary collision avoiding velocity. We then compute how much this velocity needs to be modified through time scaling to satisfy collision avoidance constraints [1]. Let this guess velocity for the i^{th} robot be represented as $\mathbf{v}_g^i$. Then we can represent $\mathbf{v}_{rvo}^i$ as

$$\mathbf{v}_{rvo}^i = s^i \mathbf{v}_g^i. \quad (2)$$

Further, let $\mathbf{v}_g^i$ lead to a position $\mathbf{p}^i$ over a short future time horizon. Then, the time scaled variant of RVO for the i^{th} robot can be represented in the following manner.

$$^{s}f^{RVO_j^i}(.) = \|\mathbf{r}^{ij}\|^2 - \frac{((\mathbf{r}^{ij})^T(2s^i\mathbf{v}_g^i - \mathbf{v}^i - \mathbf{v}^j))^2}{\|2s^i\mathbf{v}_g^i - \mathbf{v}^i - \mathbf{v}^j\|^2} - (R^{ij})^2. \quad (3)$$

Note that since, $\mathbf{v}_g^i$ and consequently $\mathbf{p}^i$ are known, the only variable in (3) is the scale factor s^i. Inequality (3) defines the space of collision avoiding velocities which are scaled version of guess velocity $\mathbf{v}_g^i$. It is clear from (2) and (3) that the solution space of (3) is a subset of the solution space of RVO constraints (1a).

It should be noted that (3) is a single variable quadratic inequality whose solution space can be characterized in closed-form [19]. It is possible to generate a lot of possible choices for $\mathbf{v}_g^i$ and solve (3) for each of them to obtain a characterization of the complete space of collision avoiding velocities $\mathbf{v}_{rvo}^i$. Each choice of $\mathbf{v}_g^i$ characterizes a path that a robot can follow to avoid collisions with a suitable velocity profile.

IV. RVOs in the Probabilistic Domain:PRVO

Let us start by representing the current trajectory of a pair of robots as the following random variables. with Gaussian distributions.

$$\mathbf{p}^i \approx N(\mu_{\mathbf{p}}^i, (\Sigma_{\mathbf{p}}^i)), \quad \mathbf{p}^j \approx N(\mu_{\mathbf{p}}^j, (\Sigma_{\mathbf{p}}^j)). \quad (4)$$

$$\mathbf{v}^i \approx N(\mu_{\mathbf{v}}^i, (\Sigma_{\mathbf{v}}^i)), \quad \mathbf{v}^j \approx N(\mu_{\mathbf{v}}^j, (\Sigma_{\mathbf{v}}^j)). \quad (5)$$

Where $\mu_{\mathbf{p}}^i, (\Sigma_{\mathbf{p}}^i), \mu_{\mathbf{v}}^i, (\Sigma_{\mathbf{v}}^i)$ and others represent position and velocity level mean and covariances, respectively. In the context of the two-robot collision scenario considered in the previous section, equations (4) and (5) model the fact that robot i has some uncertainty in the estimate of its current state and the state of the robot j. Although, we have assumed a Gaussian representation of the uncertainty, the framework presented here can also be easily extended to incorporate other representations.

Similarly, let us assume that each robot has an imperfect actuation and that there is an inherent noise between the commanded and actual velocity. This noise would result in some error between the computed and executed avoidance maneuver. Moreover, this error itself would be a random variable. In the context of RVO, we account for this uncertainty associated with the avoidance maneuver by assuming that $\mathbf{v}_{rvo}^i$ is drawn from a distribution. In other words, it is modeled as the following Gaussian random variable. The equation below models the fact that when the robot commands a velocity $\mathbf{v}_{rvo}^i$, the executed velocity can correspond to any sample drawn from a Gaussian distribution whose mean is the commanded velocity and the whose covariance is some constant $\Sigma_{\mathbf{v}_{rvo}}^i$

$$\mathbf{v}_{rvo}^i \approx N(\mathbf{v}_{rvo}^i, (\Sigma_{\mathbf{v}_{rvo}}^i)). \quad (6)$$

In light of definitions (4)-(6), $f^{RVO_j^i}(.)$ becomes a multivariate function of random variables and, consequently, a random variable itself. Thus, mathematically, constraint (1a) does not make sense. Instead, a better defined alternative would be to consider the following inequality

$$P(f^{RVO_j^i}(\mathbf{p}^i, \mathbf{p}^j, \mathbf{v}^i, \mathbf{v}^j, \mathbf{v}_{rvo}^i) \geq 0) \geq \eta. \quad (7)$$

Where, $P(.)$ represents probability. Constraint (7) ensures that the probability of RVO based collision avoidance condition (1a) being satisfied is greater than some lower bound η. In fact (7) defines the space of velocities $\mathbf{v}_{rvo}^i$ for robot i which ensures satisfaction of RVO constraints with atleast probability η for the given robot j's trajectory parameters $\mathbf{p}^j$ and $\mathbf{v}^j$.

Constraints having the general form as that of (7) are popularly known as "chance constraints" and in general, are computationally intractable [5]. The primary difficulty lies in computing the analytical form for the chance constraints. One notable exception exists in the case in which the random variables under consideration have Gaussian distribution and the chance constraints are defined over affine inequalities [6]. In such cases, efficient convex approximations for the chance constraints can be derived. However, as stated earlier, $f^{RVO_j^i}(.)$ is a non-convex quadratic in terms of random variables and thus the techniques proposed in [6] are not applicable in our case. In the next section, we present a novel solution methodology for (7) that exploits the time scaling based reformulations discussed in the previous section.

A. Overview of PRVO

Because RVO depends explicitly on both position and velocity variables, chance constraints defined over them, (7) pose unique challenges. In particular, the probability with which PRVO is satisfied depends on a complex interaction between the uncertainty associated with position and velocity variables. To elaborate this further, let us for the moment assume that there is no actuation uncertainty, i.e, each robot can perfectly execute its motion. With this assumption, let us consider figure 1(a), which shows two uncertainty region corresponding to the positions of a pair of robots at some specific time instant. Each robot's actual position can be anywhere in the uncertainty region with some probability. Moreover, each robot can have a distribution of velocities corresponding to any position sampled from their position level uncertainty region. Now, let us consider the collision scenario shown in figure 1(b) and assume that the actual position of each robot is given by a particle close to the mean. For each of these particles, let us consider two samples (shown in red and cyan) from the distribution of their current velocities. It is clear that collision avoidance is easier for the velocities shown in cyan as these are divergent velocities. In contrast, the velocities shown in red results in a difficult collision configuration. Thus, collision avoidance would be

[1] The concept of guess velocity can be thought to be similar to the notion of initial guess used to solve non-convex constraints

more likely if the more probable current velocities of the robots corresponds to the ones shown in cyan.

Based on the above example, we can conclude that, for a given position of a pair of robots, the probability of collision avoidance between them is conditioned over the distribution of their current velocities, i.e the set of probable current velocities of each robot. The effect of actuation uncertainty can be naturally appended to this insight if we model it as a distribution over commanded velocities. In other words, with actuation uncertainty, the probability of collision avoidance would be conditioned over the distribution of current and commanded velocities.

The insights deduced above are meaningful only for the given fixed position of a pair of robots. To have a complete and correct picture of the probability of collision avoidance, one needs to extend the reasoning to numerous particles sampled from the position uncertainty ellipses. Further, we also need to consider the fact that these particles themselves have a probability distribution. Nevertheless, we show that this simple idea of fixing robots positions and computing the probability of collision avoidance with respect to uncertainty in velocity variables is the main idea behind solving the chance constraints defined over RVO in an efficient manner.

V. Time Scaling Based Solution of PRVO

In this section, we first describe the motivation behind adopting a time scaling based approach and then present a detailed explanation of the solution process. To this end, recall the state and actuation uncertainty model described in (4)-(5) and (6) respectively. While both of the uncertainties have a Gaussian form, the latter i.e motion uncertainty has an added complexity. At any given instant, the state estimation uncertainty can be completely characterized (e.g. through some localization mechanism). In contrast, the mean of the motion uncertainty is unknown and can only be ascertained after one has solved some sort of collision avoidance constraints. This is a direct consequence of the fact that we have taken the unknown variable in (7) itself as a random variable to take into account the uncertainty associated with the error between the computed and the executed avoidance maneuvers.

A possible solution to the computational challenge described above, lies in the time scaling based reformulations described in previous section. Recall (3) from III-C and discussions therein which described how the solution space of $f^{RVO_j^i}(.)$ can be approximated by first choosing a guess velocity, $\mathbf{v}_g^i$ and then solving (3) which is the time scaled variant of (1a), with respect to the guess velocity. We extend a similar reasoning to the probabilistic domain.

It is clear that in the probabilistic domain, the guess velocity would not be a deterministic entity. Rather, we use the description of (6) to represent guess velocity as the following distribution.In in contrast to (6), the distribution represented by (8) is completely known because, the mean i.e $\mathbf{v}_g^i$ is the velocity that the robot chooses even before solving any collision avoidance constraints.

$$\mathbf{v}_g^i \approx N(\mathbf{v}_g^i, (\Sigma_{\mathbf{v}_g}^i)). \tag{8}$$

Now, with respect to (8), we define the following chance constraints defined over the time scaled variant of RVO, (3).

$$P({}^s f^{RVO_j^i}(\mathbf{p}^i, \mathbf{p}^j, \mathbf{v}^i, \mathbf{v}^j, s^i\mathbf{v}_g^i) \geq 0) \geq \eta. \tag{9}$$

We will refer to (9) as time scaled PRVO constraints. It can be noted that the feasible set of (9) is a subset of feasible set of constraints, (7). To be more precise, (9) defines the space of velocities that satisfy (7), but at the same time are a scaled version of the guess velocity. Similar, to the deterministic case, solving (9) for various choices for $\mathbf{v}_g^i$ can give an approximate characterization of the space of velocities which satisfy (7).

In the subsequent sections, we describe an efficient solution process for (9).

A. Solution Space of PRVO constraints

1) Bayesian Decomposition: We start by computing the following Bayesian decomposition of the left hand side of (9)

$$P({}^s f^{RVO_j^i}(\mathbf{p}^i, \mathbf{p}^j, \mathbf{v}^i, \mathbf{v}^j, s^i\mathbf{v}_g^i) \geq 0) = \int_{\mathbf{p}^j \in C^j} \int_{\mathbf{p}^i \in C^i} P({}^s f^{RVO_j^i}(.) \geq 0 | \mathbf{p}^i \in C^i, \mathbf{p}^j \in C^j) P(\mathbf{p}^j|\mathbf{p}^i) P(\mathbf{p}^i) d\mathbf{p}^i d\mathbf{p}^j . \tag{10}$$

The first term under the integral represents $P({}^s f^{RVO_j^i}(\mathbf{p}^i, \mathbf{p}^j, \mathbf{v}^i, \mathbf{v}^j, s^i\mathbf{v}_g^i) \geq 0)$ when the position variables, $(\mathbf{p}^i, \mathbf{p}^j)$ are treated as deterministic samples belonging to set C^i and C^j respectively. As we show later, the set C^i, C^j can be thought as a contour in the position uncertainty region of the robots. The second term $P(\mathbf{p}^j|\mathbf{p}^i)$ represents the distribution of position of robot j as estimated by robot i, while $P(\mathbf{p}^i)$ represents the position distribution of robot i. Clearly, the first term can be taken out of the integral since it is no longer a function of the position variables ($\mathbf{p}^i, \mathbf{p}^j$ are fixed and assume values from sets C^i and C^j respectively). Doing so, we obtain the following simplification

$$\begin{aligned} &P({}^s f^{RVO_j^i}(\mathbf{p}^i, \mathbf{p}^j, \mathbf{v}^i, \mathbf{v}^j, s^i\mathbf{v}_g^i)) \geq 0) = \\ &\quad P({}^s f^{RVO_j^i}(.) \geq 0 | \mathbf{p}^i \epsilon C^i, \mathbf{p}^j \epsilon C^j) C_j^i. \end{aligned} \tag{11}$$

$$\text{Where, } C_j^i = \int_{\mathbf{p}^j \in C^j} \int_{\mathbf{p}^i \in C^i} P(\mathbf{p}^j|\mathbf{p}^i) P(\mathbf{p}^i) d\mathbf{p}^i d\mathbf{p}^j. \tag{12}$$

Because the position distribution are known completely, the right hand side of (12) evaluates to a fixed positive constants. Now, substituting left hand side of (11) in (9), we get

$$\begin{aligned} &P({}^s f^{RVO_j^i}(\mathbf{p}^i, \mathbf{p}^j, \mathbf{v}^i, \mathbf{v}^j, s^i\mathbf{v}_g^i) \geq 0) \geq \eta. \\ &\Rightarrow P({}^s f^{RVO_j^i}(.) \geq 0 | \mathbf{p}^i \in C^i, \mathbf{p}^j \in C^j) \geq \frac{\eta}{C_j^i}. \end{aligned} \tag{13}$$

In contrast to (9), inequality (13) depends only on the velocity level random variables, while the position variables are fixed at specific values. As is evident, satisfaction of (13) ensures satisfaction of (9) and consequently original PRVO constraints (7) with atleast probability $\frac{\eta}{C_j^i}$

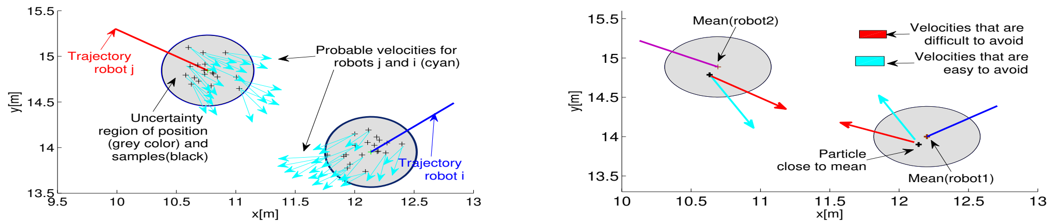

(a) (b)

Fig. 1. A conceptual description of the PRVO. Figure (a) shows a collision scenario involving two robots. The actual position of the robots can be anywhere in their respective uncertainty region (grey circles) with a particular probability. Moreover, corresponding to each position in the uncertainty region, the robots can have any velocity from a given distribution. Figure (b) shows a collision scenario where we assume that the actual position of the robots is given by particles close to the mean. Corresponding to these positions, we draw two samples (shown in red and cyan) from the distribution of the current velocities of the robots. It can be clearly seen that collision avoidance is more likely if the velocities shown in cyan represent the more probable samples. In general, the probability of collision avoidance for a fixed position is conditioned over the distribution of current and commanded velocities.

2) Surrogate Constraints: Up to this point, we have proposed a series of reformulations to convert the PRVO constraints (7) into the form given by (13). However, (13) still represents chance constraints over non-linear and non-convex inequality and is thus still challenging to solve. Thus we now, present our final reformulation which eventually leads to a closed-form characterization of the solution space of (13). The reformulation is based upon the following lemma derived from [15].

Theorem 1.

$$\textit{If,} \underset{\mathbf{p}^i \in C^i, \mathbf{p}^j \in C^j}{E}[{}^s f_{RVO^i_j}] - k\sqrt{\underset{\mathbf{p}^i \in C^i, \mathbf{p}^j \in C^j}{Var}[{}^s f_{RVO^i_j}]} \geq 0. \quad (14)$$

$$\textit{then}, \eta \geq \frac{C^i_j k^2}{1+k^2}. \quad (15)$$

Where, $\underset{\mathbf{p}^i \in C^i, \mathbf{p}^j \in C^j}{E}[.]$ and $\underset{\mathbf{p}^i \in C^i, \mathbf{p}^j \in C^j}{Var}[.]$ represents expectation and variance of the ${}^s f_{RVO^i_j}$ with respect to random variables $(\mathbf{v}^i, \mathbf{v}^j, \mathbf{v}^i_g)$, while the position variables are fixed and assume values from the set C^i and C^j. Theorem 1 essentially states that satisfaction of (14) leads to satisfaction of (9) and consequently, PRVO constraints with a lower bound probability given by 15.

Proof. From Cantelli's inequality, we have

$$P({}^s f^{RVO^i_j}(.) \geq 0 | \mathbf{p}^i \in C^i, \mathbf{p}^j \in C^j \geq \gamma^i_j) \geq \frac{k^2}{1+k^2}. \quad (16)$$

Where, $\gamma^i_j = \underset{\mathbf{p}^i \in C^i, \mathbf{p}^j \in C^j}{E}[{}^s f_{RVO^i_j}] - k\sqrt{\underset{\mathbf{p}^i \in C^i, \mathbf{p}^j \in C^j}{Var}[{}^s f_{RVO^i_j}]}$

Thus, if (14) holds, we have

$$P({}^s f^{RVO^i_j}(.) \geq 0 | \mathbf{p}^i \in C^i, \mathbf{p}^j \in C^j \geq 0) \geq \frac{k^2}{1+k^2}. \quad (17)$$

Comparing (17) with (13), we get (15).

□

Algebraic Form and Solution of Surrogate Constraints: We can compute the left hand side of (13) using symbolic packages like MATHEMATICA [18]. Now, ${}^s f^{RVO^i_j}(.)$ for fixed $\mathbf{p}^i, \mathbf{p}^j$ depends on a single variable s^i (refer (3)) that represents the scale factor by which the guess velocity $\mathbf{v}^i_g$ needs to be scaled. Thus, the surrogate constraint, (13) simplifies to following single variable quadratic inequality.

$$a^i_j (s^i)^2 + b^i_j s^i + c^i_j \geq 0. \quad (18)$$

Where, a^i_j, b^i_j, c^i_j are constants which depend on position, velocity variables, $\mathbf{p}^i, \mathbf{p}^j, \mathbf{v}^i, \mathbf{v}^j, \mathbf{v}^i_g$ and C^i_j and k. Clearly, (18) represents a single variable quadratic inequality whose solution space can be characterized in closed-form.

Summary: Thus, to summarize the discussions till now, the solution space of surrogate constraints (18) can be characterized in closed and it corresponds to that of (9) and consequently (7) for $\eta \geq C^i_j \frac{k^2}{1+k^2}$. Off course, (18) characterizes only a very small subset of collision free velocities. Nevertheless, we can always construct (18) for various choices of guess velocities $\mathbf{v}^i_g$ to obtain a good characterization of the complete space of probabilistically safe collision free velocities. Subsequently, choosing one solution from this space which optimizes some user defined metric is then straightforward.

VI. Results

A. Two Robot Benchmark

Here we validate the formulation described to this point. To this end consider figures 2(a)-2(b) and 2(c)-2(d) which show a two-robot collision scenario. For the ease of exposition, we will refer to the robots as "robot 1" and "robot 2". In the simulations presented here, each robot chooses their respective sets C^1 and C^2 to represent the 68% confidence contours from their respective uncertainty region. The value of k used to construct the inequality (14) was taken as 0.1 for the results shown in figures 2(a)-2(b), while it was fixed at 1.0 for the results shown in figures 2(c)-2(d).

Let us start by analyzing figures 2(a)-2(b). In these figures, we extract samples from the distribution of the computed velocities of each robot and then evaluate how many of these samples satisfy the RVO constraints (1a) with respect to the current velocity distribution of the other robot when the position values are drawn from the set C^1 and C^2. In other words, "robot 1" evaluates how effective is its computed avoidance maneuver with respect to current velocity distribution of "robot 2" when both its and "robot 2" position is given by the samples in set C^1 and C^2 (figure 2(a)). A similar analysis is done for "robot 2" for the current velocity distribution of "robot 1" (figure 2(b)). The velocity samples

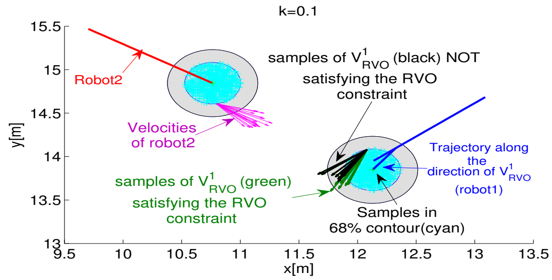

(a)

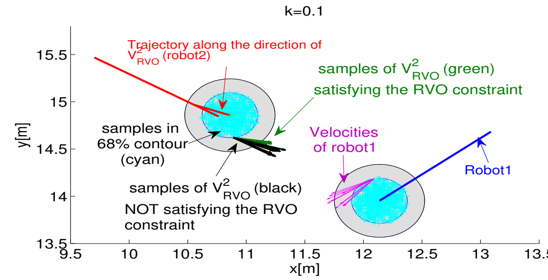

(b)

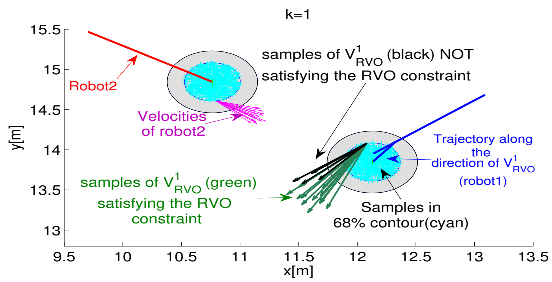

(c)

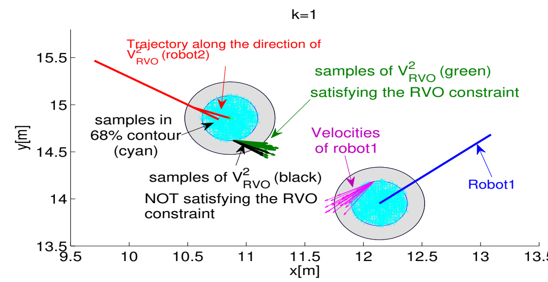

(d)

Fig. 2. Figures (a)-(d) validates the derivations presented in section V for a two robot collision scenario. The solution process starts by first fixing the position sets C^1 and C^2 for the robots. In the current case both the sets represent the 68% contour (shown in cyan) of the position uncertainty region of the robots (shown in grey). Thereafter each robots constructs inequality (14) for $k = 0.1$. To validate the effectiveness of the computed avoidance maneuver, we extract samples from the distribution of the computed velocities of each robot and evaluate how many of these samples satisfy the RVO constraints with respect to the current velocity distribution of the other robot when the position values are fixed at samples from set C^1 and C^2. The samples shown in green lead to satisfaction of RVO constraints, while those shown in black results in violation of the constraints. Now, in line of the theory presented in section V-A.2, solving (14) with increasing value of k should result in increase in probability with which RVO constraints are satisfied. This is validated in figures (c) and (d). As evident the number of samples from the distribution which leads to violation of RVO constraints has significantly reduced as compared to (a) and (b).

shown in green correspond to the ones that satisfy the RVO constraints, (1a), while those shown in black lead to the violation of (1a). We would obtain a different evaluation for each combination of position samples drawn from set C^1 and C^2. Thus, in figures 2(a)-2(b), we show the worst case result, for the position samples which gives maximum violation of the RVO constraints.

Now, in line with the theory presented in section V-A.2, solving (14) with higher values of k should lead to an increase in probability of satisfying RVO constraints, (1a). This is validated in figures 2(c)-2(d) which shows similar results as figure 2(a)-2(b), but for $k = 1.0$. An increase in probability of satisfying RVO constraints is evident by the reduction in the number of samples that lead to the violation of RVO constraints (shown in black) as compared to figure 2(a)-(2(b)).

B. Comparison with Bounding Volume Based Approaches

One of the possible approaches to account for uncertainty in a first order constraint like RVO is by constructing bounding volumes obtained by increasing the footprint of the robot by the size of the covariance of the position and velocity uncertainty. The technique has been used in several works like [17], [16]. In this section, we show that the proposed formulation is less conservative than the bounding volume based approaches. To this end, we generated 20 different problem instances with 8 robots each and compared the average arc length observed for each robot for both the proposed formulation and the bounding volume based approach. The results are summarized in figure 3(a)-3(c). From benchmarking perspective, we also present the arc lengths observed for the deterministic RVO computed using just the mean position and velocity of the robots.

The figures presents several interesting insights. Firstly, from figure 3(a), it can be seen that if only position level uncertainty is considered, then both the proposed formulation and the bounding volume based approach results in similar arc-lengths. To understand the mathematical reasoning behind this, recall the right hand side of equation (11) which under zero velocity uncertainty reduces to just C_j^i. Moreover, it can be seen from (12) that C_j^i is nothing but a contour in the position uncertainty ellipse and thus very similar to a bounding volume.

However, as velocity uncertainty (from both state estimation and actuation) is taken into account, our proposed formulation, PRVO outperforms bounding volume based approach (figures 3(b), 3(c)). On an average, we observe PRVO leads to 20% shorter paths. The variation of traversal time show similar trends. This is quantified in figure 3(d) which compares the total time required for all the robots to reach the goal position. As can be seen, PRVO takes around 33% less time. The mathematical reasoning for the this trend is as follows. The bounding volume based approach is equivalent to drawing a lot of samples from position and velocity uncertainty ellipses and writing RVO constraints with respect to each of them. However, the probability of samples play no part in shaping of the constraints. In other words, within a bounding volume, a sample close to the mean

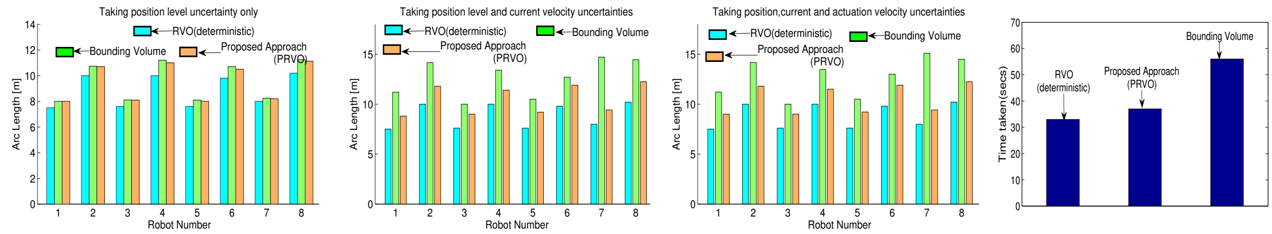

(a) (b) (c) (d)

Fig. 3. Figures (a)-(c) show arc length comparison observed across 20 problem instances with 8 robots for the proposed formulation, PRVO and the bounding volume based approach. Figure (c) presents the comparison for the total time taken for all the robots to reach the goal.

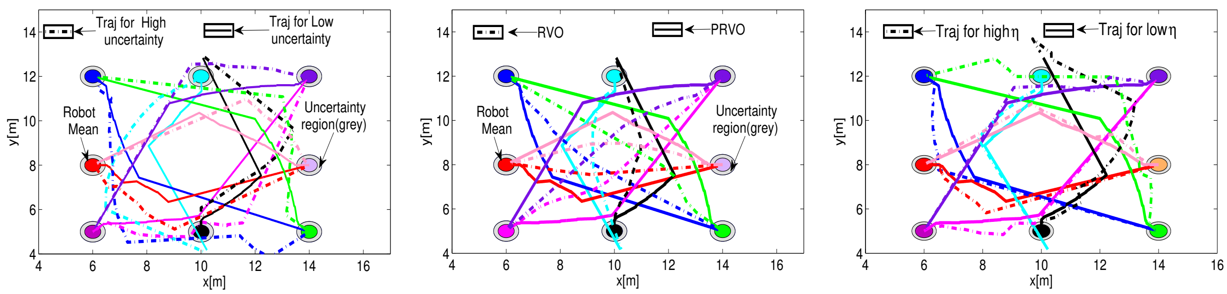

(a) (b) (c)

Fig. 4. (a): Effect of level of uncertainty on collision avoidance trajectories. (b) Comparison of deterministic RVO with PRVO for a given uncertainty. Note that while RVO trajectories are smooth, those obtained with PRVO show occasional oscillations induced by actuation uncertainty. Figure (d) shows the effect of probability of avoidance, η on collision avoidance trajectories. As can be seen, η and level of uncertainty affects collision avoidance in similar manner.

is given same importance as a sample away from the mean. This in turn leads to conservative maneuvers.

C. Effect of Uncertainty and η

Figure 4(a) shows the collision avoidance trajectories obtained from PRVO for two different uncertainty levels. The uncertainty parameters were kept same for all the robots. The low uncertainty level was characterized by $\Sigma^i_{\mathbf{p}} = diag(0.003, 0.003), \Sigma^i_{\mathbf{v}} = \Sigma^i_{\mathbf{v}_g} = diag(0.005, 0.005)$, while the high uncertainty level was characterized by $\Sigma^i_{\mathbf{p}} = diag(0.005, 0.005), \Sigma^i_{\mathbf{v}} = \Sigma^i_{\mathbf{v}_g} = diag(0.01, 0.01)$. For benchmarking purpose, we also present the comparison between PRVO and deterministic RVO in figure 4(b). The uncertainty parameters used for this figure were same as that used in figure 4(a) for trajectories corresponding to low uncertainty level.

Following points are noteworthy. Firstly, increase in uncertainty level was generally accompanied by increased deviation from straight line paths which leads each robot directly towards their goal. Moreover, increased deviation from original forward velocity profile was also observed. Secondly, note that while RVO trajectories are smooth, those obtained through PRVO show some oscillations. This is a direct consequence of actuation uncertainty which makes robot's motion imprecise and thus, a smooth transition out from the collision course cannot always be ensured.

The probability of avoidance η has a similar effect on collision avoidance as the level of uncertainty. As an example, figure 4(c) shows the trajectory plots for two different η.

D. Velocity Obstacle

In a deterministic setting, it has been shown that satisfaction of RVO constraints guarantees satisfaction of constraints

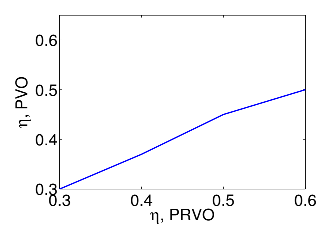

5. Figure shows an almost linear relationship between the probability of satisfaction of RVO and VO. At each η, $P({}^sf^{VO^i_j}(.) \geq 0)$ was evaluated for 20 different collision configurations and the obtained values were then averaged.

defined by Velocity Obstacle (VO), [1] [2]. To be more precise, in a two-robot collision scenario, if each each robot solves RVO constraints independently with respect to the current trajectory of the other robot, then the computed avoidance maneuvers are guaranteed to satisfy the VO constraints with respect to the new trajectory of both the robots.

Here, we empirically evaluate the validity of this mapping between RVO and VO in the probabilistic setting. We start by writing the Bayesian decomposition (10) at the VO level, for a pair of robots, (19). Note, how ${}^sf^{VO^i_j}$ depends on both s^i and s^j, which reiterates the fact that we are now computing probability of avoidance with respect to new trajectories of both the robots. In contrast, the RVO level constraints had only one variable (s^i in (10)).

$$P({}^sf^{VO^i_j}(\mathbf{p}^i, \mathbf{p}^j, s^i\mathbf{v}^i_g, s^j\mathbf{v}^j_g)) = \int_{\mathbf{p}^j \in C^j} \int_{\mathbf{p}^i \in C^i}$$
$$P({}^sf^{VO^i_j}(.) \geq 0 | \mathbf{p}^j \in C^j, \mathbf{p}^i \in C^i) P(\mathbf{p}^j|\mathbf{p}^i) P(\mathbf{p}^i) d\mathbf{p}^i d\mathbf{p}^j \quad (19)$$

We evaluated right hand side of (19) through sampling with respect to s^i and s^j obtained from solving the surrogate constraints (14) for both the robots. The sets C^i and C^j was chosen to represent 80% of the position uncertainty region of the robots. Different values of k were chosen to obtain different η. For each value of k, 20 different collision configurations were considered and right hand side of (19) was evaluated for the all the computed avoidance maneuvers. The average comparative results are summarized in figure 5 which shows the variation of $P({}^{s}f^{VO_j^i(.)} \geq 0)$ with respect to $P({}^{s}f^{RVO_j^i(.)} \geq 0)$. As can be seen, we observe an almost linear relationship between the two. This points to a strong correlation between probability of satisfaction of RVO and VO constraints.

E. Computation Time

As explained in section V, the solution process requires each robot to first choose a guess velocity $\mathbf{v}_g^i$. Then, surrogate constraints (14) are constructed with respect to the guess velocities and solved to obtain the scale factor s^i. Thus, computation time of our proposed algorithm can be represented by the following expression

$$T_{comp} = N_{\mathbf{v}_g^i} T_{surrogate}. \tag{20}$$

Where, $N_{\mathbf{v}_g^i}$ represents the number of possible values of $\mathbf{v}_g^i$ that the robot needs to evaluate to obtain a solution space, while, $T_{surrogate}$ represents the computation time required to solve (14) with respect to the neighboring robots. Figure 6(a) shows the plot of $N_{\mathbf{v}_g^i}$ as a function of the number of neighboring robots. The plot of total computation time T_{comp} is shown in figure. The value of $T_{surrogate}$ can be obtained from the plot following (20). It should be noted that computation times are provided for an unoptimized Matlab implementation on a laptop with $i7$ processor and 8GB of RAM,. Since, (14) is a single variable quadratic inequality, its solution space with respect to n neighboring robots can be computed by a simple sorting algorithm. A C^{++} implementation of our algorithm is expected to be much faster.

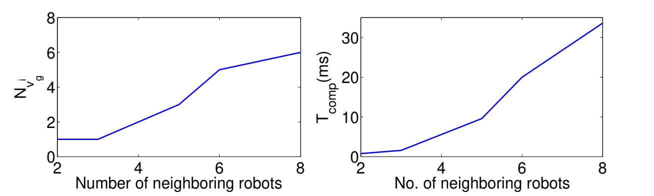

(a) (b)

Fig. 6. (a): Number of possible values of $\mathbf{v}_g^i$ that the robot needs to evaluate to obtain a solution space (b): Total computation time.

VII. Conclusions, Limitations and Future Work

In this paper, we used the concept of chance constraints to derive PRVO, a probabilistic variant of RVO. The extremely difficult chance constraints were made computationally tractable by a series of novel reformulations based on Bayesian decomposition and time scaling concepts. Eventually, a closed-form characterization of collision free velocities for a specified lower bound probability was obtained.We validated our formulations through extensive numerical simulations highlighting the effect of uncertainty and at the time showing an improvement over the existing bounding volume based approaches in terms of arc lengths and traversal times.

The current work was designed for simple single integrator systems. The future efforts will thus be focused towards relaxing this limitation and extending the algorithm to higher order as well non-holonomic kino-dynamic systems. A part of the efficiency of our approach is due to the Gaussian representation of uncertainty. In particular, the algebraic form of surrogate constraints depends critically on it. Thus, it would be interesting to analyze the proposed approach with respect to different representations of uncertainty.

References

[1] Fiorini, Paolo, and Zvi Shiller. "Motion planning in dynamic environments using velocity obstacles." The International Journal of Robotics Research 17, no. 7 (1998): 760-772.

[2] Van den Berg, Jur, Ming Lin, and Dinesh Manocha. "Reciprocal velocity obstacles for real-time multi-agent navigation." In Robotics and Automation, 2008. ICRA 2008. IEEE International Conference on, pp. 1928-1935. IEEE, 2008.

[3] Alonso-Mora, Javier, Andreas Breitenmoser, Martin Rufli, Paul Beardsley, and Roland Siegwart. "Optimal reciprocal collision avoidance for multiple non-holonomic robots." In Distributed Autonomous Robotic Systems, pp. 203-216. Springer Berlin Heidelberg, 2013.

[4] Van Den Berg, Jur, Stephen J. Guy, Ming Lin, and Dinesh Manocha. "Reciprocal n-body collision avoidance." In Robotics research, pp. 3-19. Springer Berlin Heidelberg, 2011.

[5] Nemirovski, Arkadi. "On safe tractable approximations of chance constraints." European Journal of Operational Research 219, no. 3 (2012): 707-718.

[6] Boyd, Stephen. "Chance-constrained optimization." (2015).

[7] Kluge, B., and Prassler, E. (2006, January). Recursive probabilistic velocity obstacles for reflective navigation. In Field and Service Robotics (pp. 71-79). Springer Berlin Heidelberg.

[8] Fulgenzi, C., Tay, C., Spalanzani, A., and Laugier, C. (2008, September). Probabilistic navigation in dynamic environment using rapidly-exploring random trees and gaussian processes. In Proc. IEEE IROS 2008 (pp. 1056-1062).

[9] Kushleyev, A., and Likhachev, M. Time-bounded lattice for efficient planning in dynamic environments. In Proc. of IEEE ICRA 2009 (pp. 1662-1668).

[10] Luders, Brandon, Mangal Kothari, and Jonathan P. How. "Chance constrained RRT for probabilistic robustness to environmental uncertainty." In AIAA guidance, navigation, and control conference (GNC), Toronto, Canada. 2010.

[11] Du Toit, Noel E., and Joel W. Burdick. "Robot motion planning in dynamic, uncertain environments." IEEE Transactions on Robotics 28, no. 1 (2012): 101-115.

[12] Van Den Berg, Jur, Pieter Abbeel, and Ken Goldberg. "LQG-MP: Optimized path planning for robots with motion uncertainty and imperfect state information." The International Journal of Robotics Research 30, no. 7 (2011): 895-913.

[13] Lyons, Daniel, Jan-P. Calliess, and Uwe D. Hanebeck. "Chance constrained model predictive control for multi-agent systems with coupling constraints." In American Control Conference (ACC), 2012, pp. 1223-1230. IEEE, 2012.

[14] Fiorini, Paolo, and Zvi Shiller. "Motion planning in dynamic environments using velocity obstacles." The International Journal of Robotics Research 17, no. 7 (1998): 760-772.

[15] Gopalakrishnan, Bharath, Arun Kumar Singh, and K. Madhava Krishna. "closed-form characterization of collision free velocities and confidence bounds for non-holonomic robots in uncertain dynamic environments." In Intelligent Robots and Systems (IROS), 2015 IEEE/RSJ International Conference on, pp. 4961-4968. IEEE, 2015.

[16] Snape, J., van den Berg, J., Guy, S. J., and Manocha, D. (2011). The hybrid reciprocal velocity obstacle. Robotics, IEEE Transactions on, 27(4), 696-706.

[17] Claes, Daniel, Daniel Hennes, Karl Tuyls, and Wim Meeussen. "Collision avoidance under bounded localization uncertainty." In 2012 IEEE/RSJ International Conference on Intelligent Robots and Systems, pp. 1192-1198. IEEE, 2012.

[18] Wolfram, S. (2009). Mathematica. Wolfram Research, Champaign.

[19] Gopalakrishnan, Bharath, Arun Kumar Singh, and K. Madhava Krishna. "Time scaled collision cone based trajectory optimization approach for reactive planning in dynamic environments." In 2014 IEEE/RSJ International Conference on Intelligent Robots and Systems, pp. 4169-4176. IEEE, 2014.